APL Photonics

RESEARCH ARTICLE | SEPTEMBER 10 2025

# Sparse optimization of two-dimensional terahertz spectroscopy

Z. Wang ; H. Da ; A. S. Disa ; T. Pullerits ; A. Liu ; F. Schlawin



*APL Photonics* 10, 096107 (2025)
https://doi.org/10.1063/5.0276901

# Sparse optimization of two-dimensional terahertz spectroscopy

Cite as: APL Photon. 10, 096107 (2025); doi: 10.1063/5.0276901
Submitted: 21 April 2025 • Accepted: 21 August 2025 •
Published Online: 10 September 2025



Z. Wang,[1,2,3] H. Da,[4] A. S. Disa,[5] T. Pullerits,[6] A. Liu,[7,a)] and F. Schlawin[1,2,8,a)]

## AFFILIATIONS

[1] Max Planck Institute for the Structure and Dynamics of Matter, Hamburg, Germany
[2] University of Hamburg, Luruper Chaussee 149, Hamburg, Germany
[3] Department of Physics, Stockholm University, Albanova University Centre, SE-106 91 Stockholm, Sweden
[4] CNPC Research Institute of Safety and Environment Technology, Beijing 102206, China
[5] School of Engineering and Applied Physics, Cornell University, Ithaca, New York 14853, USA
[6] Department of Chemical Physics, Lund University, P.O. Box 124, Lund 22100, Sweden
[7] Condensed Matter Physics and Materials Science Division, Brookhaven National Laboratory, Upton, New York 11973-5000, USA
[8] The Hamburg Centre for Ultrafast Imaging, Hamburg, Germany

[a)] **Authors to whom correspondence should be addressed:** aliu1@bnl.gov and frank.schlawin@uni-hamburg.de

## ABSTRACT

Two-dimensional terahertz spectroscopy (2DTS) is a low-frequency analog of two-dimensional optical spectroscopy that is rapidly maturing as a probe of a wide variety of condensed matter systems. However, a persistent problem with 2DTS is the long experimental acquisition times, which prevent its broader adoption. A potential solution, requiring no increase in experimental complexity, is signal reconstruction via compressive sensing. In this work, we apply the sparse exponential mode analysis (SEMA) technique to 2DTS of a cuprate superconductor. We benchmark the performance of the algorithm in reconstructing terahertz nonlinearities and find that SEMA reproduces the asymmetric photon echo line shapes at sampling rates as low as 10%, reaching the reconstruction noise floor at sampling rates beyond 20%–30%. The success of SEMA in reproducing such subtle, asymmetric line shapes confirms compressive sensing as a general method to accelerate 2DTS and multidimensional spectroscopies more broadly.



Multidimensional coherent spectroscopies[1–3] have revolutionized our understanding of complex systems ranging from molecular liquids[4–7] to quantum-confined nanostructures[8–10] and even biological complexes.[11–14] In recent years, two-dimensional terahertz spectroscopy (2DTS)[15,16] has brought the unique capabilities of multidimensional techniques to condensed matter systems,[17] in which many fundamental excitations can be found at low energies.[18,19] Recent such experiments have studied, for example, ferroelectrics,[20,21] ferromagnets,[22,23] and even superconductors.[24,25] However, the technique of 2DTS is still in a nascent stage, with insufficient acquisition efficiencies remaining an obstacle to studying materials with small nonlinear optical signals.

At optical and infrared frequencies and in nuclear magnetic resonance, there has been tremendous effort in accelerating multidimensional spectroscopic techniques.[26–28] Yet the need to accelerate 2DTS is even more pressing, since unique challenges such as long data acquisition (with reported acquisition times reaching one week for a single spectrum[29]) and potential degradation of terahertz generation over time[30] restrict the range of applications. Currently, the primary method for accelerating 2DTS is single-shot THz detection,[31] where the entire THz waveform is captured simultaneously. There are various methods to implement single-shot detection schemes,[32] but all of them inevitably increase experimental complexity and have their unique trade-offs. Other methods of accelerating 2DTS are, therefore, desirable.

In contrast to increasing signal acquisition rate, an alternative approach to accelerating 2DTS is to reduce the requirements for signal acquisition itself. For a signal sampled uniformly in time, it is well known[33] that the Nyquist criterion requires a minimum sampling rate of twice the signal frequency. However, one may

circumvent this limit by non-uniform sampling and subsequent signal reconstruction via compressive sensing algorithms.[34–37] So far, compressive sensing has been successfully demonstrated not only in ultrafast spectroscopy[38] but also in multidimensional NMR[39] and multidimensional optical spectroscopies.[40–43] However, these techniques have yet to be applied toward 2DTS, which stands to benefit even more from acceleration. Compressive sensing has also not been applied to asymmetric two-dimensional spectral line shapes, which are frequently encountered in disordered systems[43,44] and strong vibronic coupling[45,46] more generally. Here, we address these two open problems and implement the sparse exponential mode analysis (SEMA) method based on dictionary learning, which has been described in detail elsewhere.[41,42] In short, the SEMA algorithm approximates the signal as a superposition of multiple sparse components, each characterized by frequency, damping coefficient, and complex amplitude. In the code, the dictionary matrix $A$ is composed of products of sparse signals in two dimensions, expressed as damped exponentials, $\exp(j2\pi t_1\omega_1 - t_1\beta_1) * \exp(j2\pi t_2\omega_2 - t_2\beta_2)$, where $t_1$ and $t_2$ are sampling times, $\omega_1$ and $\omega_2$ are frequencies, and $\beta_1$ and $\beta_2$ are damping coefficients. We first initialize a dictionary that covers only the frequency dimension, with damping coefficients set to zero. This dictionary is then iteratively optimized by updating frequencies and damping coefficients based on residuals. Signal space coverage is ensured by the initial frequency range and dynamic grid optimization. We choose the SEMA method as it not only requires fewer data points than traditional compressive sensing methods such as LASSO and matching pursuit, but also can reconstruct both resonance frequencies and linewidths simultaneously.

As an ideal test case, we apply SEMA toward reconstructing the 2DTS spectra of the Josephson plasma resonance[47] in the optimally doped cuprate superconductor $La_{1.83}Sr_{0.17}CuO_4$ (LSCO), which has a plasma frequency $f_p = 2$ THz. The experiment is schematically shown in Fig. 1(a), in which 2 THz excitation pulses ($E_A$ and $E_B$) polarized along the c-axis of LSCO drive interlayer supercurrents that radiate a nonlinear optical signal $E_{NL}$ as a function of inter-pulse time delay $\tau$ and electro-optic sampling (EOS) time t. In particular, we measure the "Josephson echo" signal, which has previously been used[25] to measure disordered superconductivity in this same compound, exhibiting an asymmetric "almond-shaped" spectral line shape. Traditional compressive sensing methods fail to accurately reconstruct such complex features at low sampling rates,[41] and we thus chose it specifically to test the capabilities of SEMA. Briefly, the echo nonlinearity arises from initial supercurrents driven by $E_B$ that subsequently undergo a time-reversal operation induced by $E_A$, resulting in its oppositely signed coordinates in frequency space.[43] The underlying wavevector phase-matching condition that isolates the echo signal has been described elsewhere.[25]

In Fig. 1(b), we describe the two time-domain acquisition schemes for generating a 2DTS spectrum. On the left, we depict conventional Fourier sampling of $E_{NL}$ with a uniform sampling grid, where the time step determines the frequency bandwidth and the time range determines the frequency resolution. On the right, we

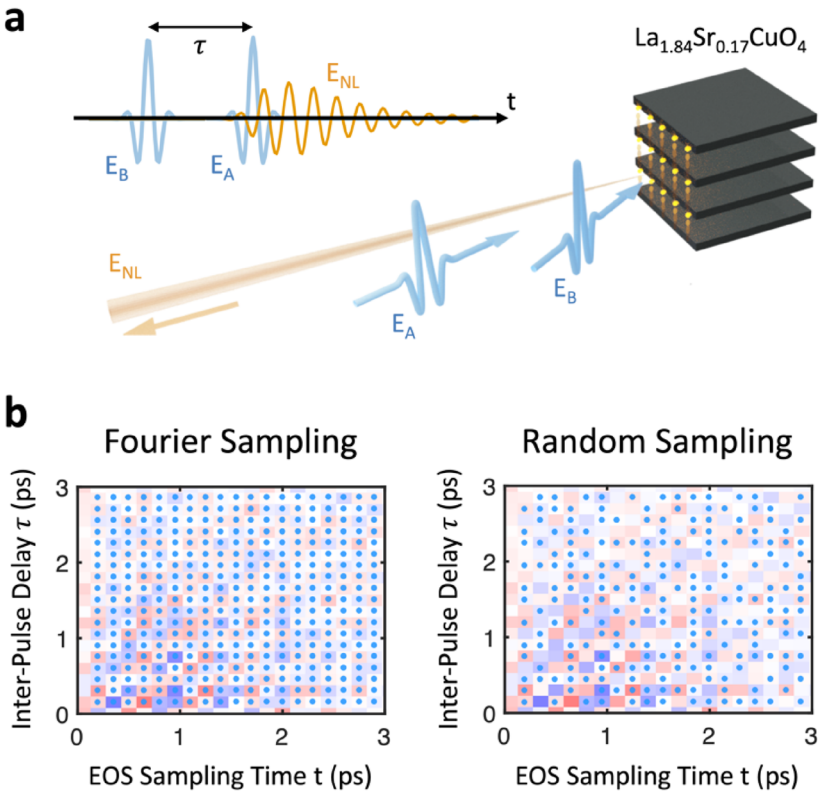


**FIG. 1. Random sampling in two-dimensional terahertz spectroscopy.** (a) Schematic of the 2DTS measurement, in which two excitation fields $E_A$ and $E_B$ cooperatively drive nonlinearities of the Josephson plasma resonance in optimally doped $La_{1.84}Sr_{0.17}CuO_4$. The resulting supercurrents radiate a nonlinear electric field $E_{NL}$, which is measured as a function of the inter-pulse time delay $\tau$ and the laboratory time t as shown in the inset. (b) Two possible acquisition schemes of the nonlinear signal $E_{NL}$, where sampled data points are indicated by blue dots. (Left) A uniform sampling grid appropriate for Fourier transform into the frequency-domain. (Right) Non-uniform sampling appropriate for reconstruction via compressive sensing algorithms.

depict sparse sampling of $E_{NL}$, where the signal is randomly sampled across the same temporal range, generally with far fewer data points. In this case, as shown by Candès *et al.*,[35] the Nyquist criterion may be circumvented using appropriate reconstruction algorithms.

We begin by measuring the Josephson echo signal at a temperature of 6 K (the lowest temperature chosen to maximize peak asymmetry) via Fourier sampling, as shown in Fig. 2(a). The signal is sampled over time ranges of 6.9 and 7.95 ps along $\tau$ and t, respectively (chosen to cover the entire signal decay), with identical time steps of 150 fs, resulting in 46 × 53 = 2438 total sampled data points before zero-padding by twice the sampling size[7] and a total acquisition time of ~3 h. We then use the SEMA algorithm to reconstruct the signal, which fits a sparsely sampled dataset to a dictionary of frequencies and spectral linewidths. This dictionary is iteratively refined, until convergence is reached[41,42] (note that the algorithm need not be trained on a dataset before its reconstruction). To investigate the accuracy of the SEMA reconstruction method, we non-uniformly sample a fraction of the Fourier-sampled dataset as an input to our compressive sensing algorithm for subsequent reconstruction. The reconstructed time-domain signal is shown in Fig. 2(b) for representative sampling of 5% and 15% of the original dataset, which exhibit qualitative differences. While the reconstruction with 5% of the data can be seen to reproduce the oscillation frequencies and their relative phase along each time axis, the reconstruction of 15% more accurately reproduces the oscillation lifetimes of the Josephson echo signal. To more easily infer the reconstruction accuracy, it is instructive to examine the spectral line shapes of the Josephson echo signal in the frequency domain.

In Fig. 3, we show the 2DTS spectra obtained by Fourier transform of the time-domain data in Fig. 2 into the frequency domain. Fourier transform of the original Fourier-sampled signal (with zero-padding by twice the sampling size) returns the asymmetric "almond-shaped" peak shown in Fig. 3(a), indicative of a disordered Josephson plasma resonance as discussed in Ref. 25. In

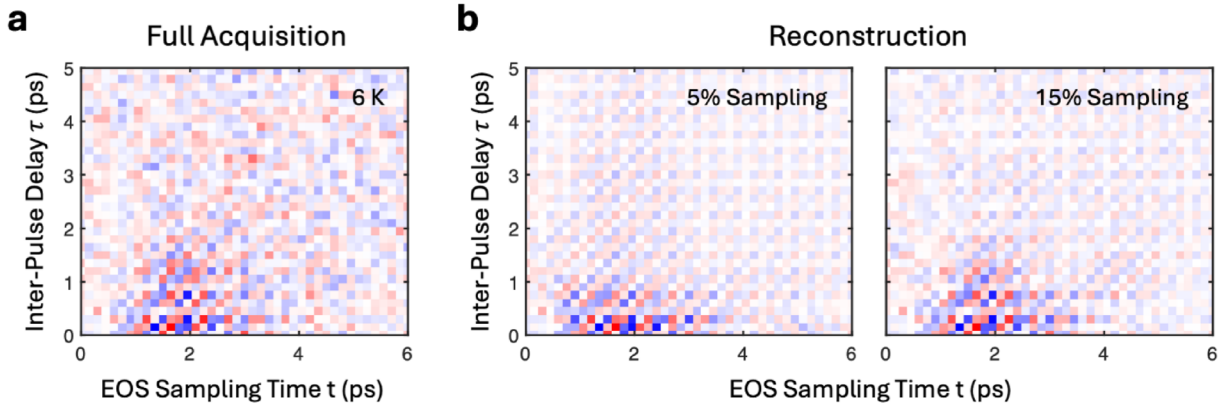


**FIG. 2. Time-domain compressive sensing.** (a) Fourier-sampled Josephson echo signal (at a sample temperature of 6 K) in the time domain. (b) Reconstructions of the Josephson echo signal at the same time coordinates $\{\tau, t\}$ from sparse sampling of 5% and 15% of the data points in (a). More accurate reconstruction is qualitatively evident with increasing sampling percentage.

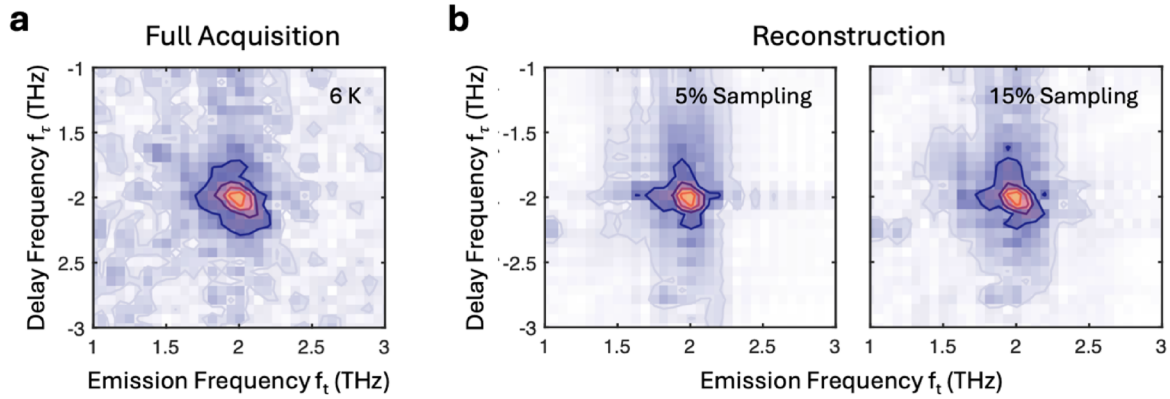


**FIG. 3. Frequency-domain compressive sensing.** (a) Reference 2DTS spectrum acquired by Fourier transform of the Fourier sampled time-domain data in Fig. 2(a). (b) Reconstructed 2DTS spectra acquired by Fourier transform of the reconstructed time-domain data in Fig. 2(b). At 5% sampling, a symmetric peak is observed, while increasing sampling percentage retrieves the asymmetric "echo" line shape.

comparison, Fourier transform of the reconstructed time-domain data reveals a strong dependence on the percentage of data used for reconstruction. The reconstruction of 5% exhibits a cross-shaped peak typical of a homogeneously broadened resonance,[43] while the reconstruction of 15% qualitatively reproduces the true asymmetric line shape.

We now examine the accuracy of the reconstructed two-dimensional line shapes more closely. Slices of both the Fourier-sampled and reconstructed 2DTS spectra are taken along the "diagonal" ($|f_t| = |f_\tau|$) and perpendicular "cross-diagonal" directions used to characterize intrinsic and disorder broadening.[43] The comparison between slices taken from the full Fourier-sampled spectrum and those taken from the 5% reconstruction is shown in Fig. 4(a), where we see that the reconstruction is less accurate and returns similar linewidths in both directions. The reconstruction further misses the non-Lorentzian tails of the resonance entirely. However, as shown in Fig. 4(b), increasing the sampling percentage to 15% results in a reconstruction that accurately reproduces not only both linewidths but also subtle details of the fully sampled spectral line shapes.

Finally, we quantify the reconstruction accuracy by considering the residual error of each reconstruction. We obtain residual maps of the 2DTS spectra by subtracting the reconstructed spectra from the fully sampled spectra, which are then normalized to the maximum amplitude of the fully sampled spectra and are plotted in Fig. 5(a). We note that the residual map of the 5% sampling spectrum exhibits

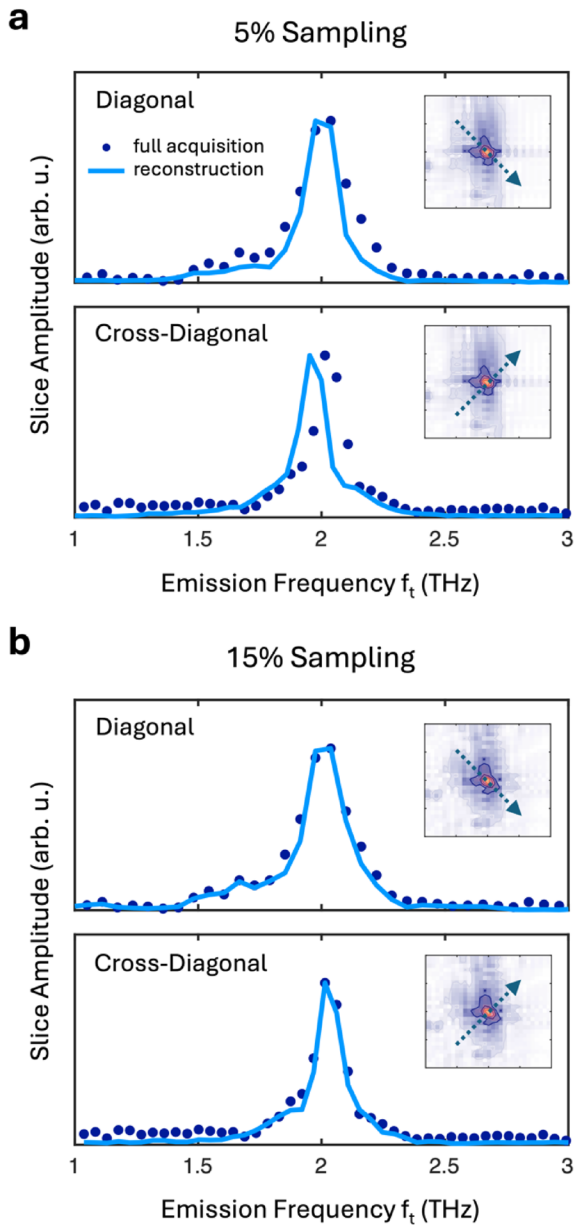


**FIG. 4. Reconstructed line shapes.** Comparison of cross sections taken (indicated inset) from the original reference 2DTS spectrum with those taken from the 2DTS spectra reconstructed from (a) 5% sampling and (b) 15% sampling.

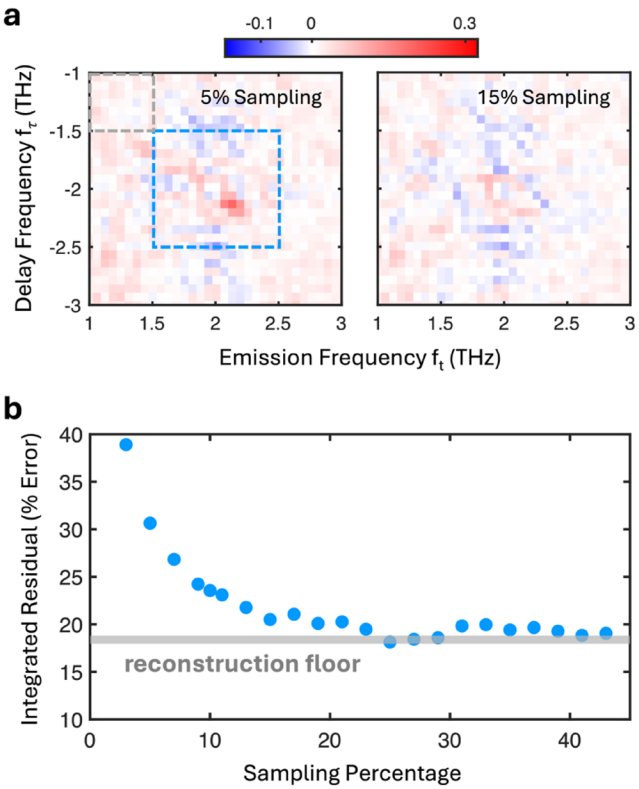


**FIG. 5. Reconstruction residual error.** (a) Residual error of the reconstructions found by subtracting the reference spectrum from the reconstructed spectra at sampling percentages of 5% and 15% and normalizing to the maximum amplitude of the reference spectrum. (b) Integrated error found by summing the (unnormalized) magnitude of the residual error across the region marked by the blue dashed box in the left panel of (a) and normalizing to the integrated value of the reference spectrum across the same frequency range. The error for each sampling percentage shown is the average of 100 reconstructions. The indicated reconstruction noise floor is found by performing the same procedure for the region marked by the gray dashed box in the left panel of (a), in which no signal is present, and scaling by an area factor of 4.

a significant structure, with positive (red) errors near the peak center and negative (blue) errors in the wings of the peak. However, the residual map of the 15% sampling spectrum exhibits a much weaker structure with only negative (blue) errors in the wings remaining apart from the reconstruction noise. This is supported by the integrated residual error shown in Fig. 5(b), which approaches the noise floor with increasing sampling percentage as expected. Beyond 30% sampling, the reconstruction accuracy at this sampling percentage is primarily limited by the measurement signal-to-noise ratio.

Having demonstrated compressive sensing as a viable method to reconstruct 2DTS spectra, we now turn to an outlook for its application to real experimental scenarios. In the results presented here, we find an approximate lower limit of 10% sampling for accurate reconstruction (5% error above the reconstruction noise floor) of the 2DTS spectrum and further reach the reconstruction noise floor above 20%–30% sampling. However, we emphasize that the Josephson echo signal considered here exhibits a more complicated spectral line shape than most other 2DTS signals reported to date. For reconstructing symmetric "non-rephasing" signals, signals from systems with multiple resonances/coupling, or signals from homogeneously broadened systems more generally, we expect these limits on the sampling percentage to be relaxed even further. Finally, we emphasize that these sparse sampling techniques can be applied to data acquired via any experimental protocols for 2DTS. Combining such sparse optimization with other techniques such as single-shot THz detection[31] will therefore bring a new level of versatility to 2DTS techniques, enabling the study of systems with weak optical nonlinearities and fragile systems sensitive to external perturbation. Further algorithmic developments and constrained random sampling[48] may also yield additional performance improvements.

The supplementary material contains details on the compressive sensing algorithm, expanded reconstruction data, and the experimental setup that was used to generate data in this paper.

We greatly appreciate Andreas Jakobsson's previous help with theory, Andrea Cavalleri for the use of 2DTS data measured at the Max Planck Institute of Structure and Dynamics of Matter, and Dieter Jaksch and Markus Kowalewski for fruitful discussions. Z.W. acknowledges support from the Swedish Research Council VR (Grant No. 2022–06176). F.S. acknowledges support from the Cluster of Excellence "Advanced Imaging of Matter" of the Deutsche Forschungsgemeinschaft (DFG)—EXC 2056—Project ID 390715994. The work at BNL was supported by the U.S. Department of Energy (DOE), Office of Basic Energy Sciences (BES), under Contract No. DOE-SC0012704. The work at Lund University was supported by the Swedish Research Council (2021-05207) and Swedish Energy Agency (50709-1).

## AUTHOR DECLARATIONS

### Conflict of Interest

The authors have no conflicts to disclose.

### Author Contributions

**Z. Wang**: Conceptualization (supporting); Formal analysis (lead); Project administration (lead); Writing – original draft (supporting). **H. Da**: Formal analysis (equal). **A. S. Disa**: Data curation (supporting); Writing – review & editing (supporting). **T. Pullerits**: Formal analysis (supporting); Writing – review & editing (equal). **A. Liu**: Conceptualization (equal); Formal analysis (equal); Writing – original draft (equal). **F. Schlawin**: Conceptualization (equal); Supervision (equal); Writing – review & editing (equal).

## DATA AVAILABILITY

The data that support the findings of this study are available from the corresponding authors upon reasonable request.

## REFERENCES

[1] S. T. Cundiff and S. Mukamel, "Optical multidimensional coherent spectroscopy," Phys. Today **66**(7), 44–49 (2013).
[2] S. Mukamel, *Principles of Nonlinear Optical Spectroscopy* (Oxford University Press, 1999).
[3] D. M. Jonas, "Two-dimensional femtosecond spectroscopy," Annu. Rev. Phys. Chem. **54**(1), 425–463 (2003).
[4] M. Cho, "Coherent two-dimensional optical spectroscopy," Chem. Rev. **108**(4), 1331–1418 (2008).
[5] C. Kolano, J. Helbing, M. Kozinski, W. Sander, and P. Hamm, "Watching hydrogen-bond dynamics in a β-turn by transient two-dimensional infrared spectroscopy," Nature **444**(7118), 469–472 (2006).
[6] S. Biswas, J. Kim, X. Zhang, and G. D. Scholes, "Coherent two-dimensional and broadband electronic spectroscopies," Chem. Rev. **122**(3), 4257–4321 (2022).
[7] P. Hamm and M. Zanni, *Concepts and Methods of 2D Infrared Spectroscopy* (Cambridge University Press, 2011).
[8] A. Liu, D. B. Almeida, L. A. Padilha, and S. T. Cundiff, "Perspective: Multidimensional coherent spectroscopy of perovskite nanocrystals," J. Phys. Mater. **5**(2), 021002 (2022).
[9] E. Amarotti, Z. Wang, A. Hedse, N. Lenngren, K. Žídek, K. Zheng, D. Zigmantas, and T. Pullerits, "Direct visualization of confinement and many-body correlation effects in 2D spectroscopy of quantum dots," Adv. Opt. Mater. **12**(15), 2302968 (2024).
[10] H. Li, B. Lomsadze, G. Moody, C. Smallwood, and S. T. Cundiff, *Optical Multidimensional Coherent Spectroscopy* (Oxford University Press, 2023).
[11] A. Chenu and G. D. Scholes, "Coherence in energy transfer and photosynthesis," Annu. Rev. Phys. Chem. **66**, 69–96 (2015).
[12] T. Brixner, J. Stenger, H. M. Vaswani, M. Cho, R. E. Blankenship, and G. R. Fleming, "Two-dimensional spectroscopy of electronic couplings in photosynthesis," Nature **434**(7033), 625–628 (2005).
[13] G. D. Scholes, G. R. Fleming, L. X. Chen, A. Aspuru-Guzik, A. Buchleitner, D. F. Coker, G. S. Engel, R. van Grondelle, A. Ishizaki, D. M. Jonas, J. S. Lundeen, J. K. McCusker, S. Mukamel, J. P. Ogilvie, A. Olaya-Castro, M. A. Ratner *et al.*, "Using coherence to enhance function in chemical and biophysical systems," Nature **543**(7647), 647–656 (2017).
[14] F. D. Fuller, J. Pan, A. Gelzinis, V. Butkus, S. S. Senlik, D. E. Wilcox, C. F. Yocum, L. Valkunas, D. Abramavicius, and J. P. Ogilvie, "Vibronic coherence in oxygenic photosynthesis," Nat. Chem. **6**(8), 706–711 (2014).
[15] J. Lu and K. Nelson, "Two-dimensional spectroscopy at terahertz frequencies," in *Multidimensional Time-Resolved Spectroscopy* (Springer, 2018), pp. 275–320.
[16] A. Liu and A. Disa, "Excitation-dependent features and artifacts in 2-D terahertz spectroscopy," Opt. Express **32**(16), 28160–28168 (2024).
[17] A. Liu, "Multidimensional terahertz probes of quantum materials," npj Quantum Mater. **10**(1), 18 (2025).
[18] D. Nicoletti and A. Cavalleri, "Nonlinear light–matter interaction at terahertz frequencies," Adv. Opt. Photonics **8**(3), 401–464 (2016).
[19] D. N. Basov, R. D. Averitt, D. van der Marel, M. Dressel, and K. Haule, "Electrodynamics of correlated electron materials," Rev. Mod. Phys. **83**(2), 471 (2011).

[20]S. Pal, N. Strkalj, C.-J. Yang, M. C. Weber, M. Trassin, M. Woerner, and M. Fiebig, "Origin of terahertz soft-mode nonlinearities in ferroelectric perovskites," Phys. Rev. X **11**(2), 021023 (2021).
[21]H.-W. Lin, G. Mead, and G. A. Blake, "Mapping $LiNbO_3$ phonon-polariton nonlinearities with 2D THz-THz-Raman spectroscopy," Phys. Rev. Lett. **129**(20), 207401 (2022).
[22]Z. Zhang, F. Y. Gao, J. B. Curtis, Z.-J. Liu, Y.-C. Chien, A. von Hoegen, M. T. Wong, T. Kurihara, T. Suemoto, P. Narang, E. Baldini, and K. A. Nelson, "Terahertz field-induced nonlinear coupling of two magnon modes in an antiferromagnet," Nat. Phys. **20**, 801–806 (2024).
[23]C. Huang, L. Luo, M. Mootz, J. Shang, P. Man, L. Su, I. E. Perakis, Y. X. Yao, A. Wu, and J. Wang, "Extreme terahertz magnon multiplication induced by resonant magnetic pulse pairs," Nat. Commun. **15**(1), 3214 (2024).
[24]L. Luo, M. Mootz, J. H. Kang, C. Huang, K. Eom, J. W. Lee, C. Vaswani, Y. G. Collantes, E. E. Hellstrom, I. E. Perakis, C. B. Eom, and J. Wang, "Quantum coherence tomography of light-controlled superconductivity," Nat. Phys. **19**, 201–209 (2022).
[25]A. Liu, D. Pavićević, M. H. Michael, A. G. Salvador, P. E. Dolgirev, M. Fechner, A. S. Disa, P. M. Lozano, Q. Li, G. D. Gu, E. Demler, and A. Cavalleri, "Probing inhomogeneous cuprate superconductivity by terahertz Josephson echo spectroscopy," Nat. Phys. **20**(11), 1751–1756 (2024).
[26]X. Qu, Y. Huang, H. Lu, T. Qiu, D. Guo, T. Agback, V. Orekhov, and Z. Chen, "Accelerated nuclear magnetic resonance spectroscopy with deep learning," Angew. Chem., Int. Ed. **59**(26), 10297–10300 (2020).
[27]J. N. Sanders, S. K. Saikin, S. Mostame, X. Andrade, J. R. Widom, A. H. Marcus, and A. Aspuru-Guzik, "Compressed sensing for multidimensional spectroscopy experiments," J. Phys. Chem. Lett. **3**(18), 2697–2702 (2012).
[28]S. Roeding, N. Klimovich, and T. Brixner, "Optimizing sparse sampling for 2D electronic spectroscopy," J. Chem. Phys. **146**(8), 084201 (2017).
[29]J. Lu, Y. Zhang, H. Y. Hwang, B. K. Ofori-Okai *et al.*, "Nonlinear two-dimensional terahertz photon echo and rotational spectroscopy in the gas phase," Proc. Natl. Acad. Sci. U. S. A. **113**(42), 11800–11805 (2016).
[30]M. Jazbinsek, U. Puc, A. Abina, and A. Zidansek, "Organic crystals for THz photonics," Appl. Sci. **9**(5), 882 (2019).
[31]F. Y. Gao, Z. Zhang, Z.-J. Liu, and K. A. Nelson, "High-speed two-dimensional terahertz spectroscopy with echelon-based shot-to-shot balanced detection," Opt. Lett. **47**(14), 3479–3482 (2022).
[32]S. M. Teo, B. K. Ofori-Okai, C. A. Werley, and K. A. Nelson, "Invited Article: Single-shot THz detection techniques optimized for multidimensional THz spectroscopy," Rev. Sci. Instrum. **86**(5), 051301 (2015).
[33]J. G. Proakis and D. G. Manolakis, *Digital Signal Processing: Principles, Algorithms and Applications* (Pearson, 2021).
[34]M. Rani, S. B. Dhok, and R. B. Deshmukh, "A systematic review of compressive sensing: Concepts, implementations and applications," IEEE Access **6**, 4875–4894 (2018).
[35]E. Candès, J. Romberg, and T. Tao, "Stable signal recovery from incomplete and inaccurate measurements," Commun. Pure Appl. Math. **59**(8), 1207–1223 (2006).
[36]D. L. Donoho, "Compressed sensing," IEEE Trans. Inf. Theory **52**(4), 1289–1306 (2006).
[37]E. J. Candes and M. B. Wakin, "An introduction to compressive sampling," IEEE Signal Process. Mag. **25**(2), 21–30 (2008).
[38]S. Adhikari, C. L. Cortes, X. Wen, S. Panuganti, D. J. Gosztola, R. D. Schaller, G. P. Wiederrecht, and S. K. Gray, "Accelerating ultrafast spectroscopy with compressive sensing," Phys. Rev. Appl. **15**(2), 024032 (2021).
[39]J. C. Ye, "Compressed sensing MRI: A review from signal processing perspective," BMC Biomed. Eng. **1**(1), 8 (2019).
[40]J. A. Dunbar, D. G. Osborne, J. M. Anna, and K. J. Kubarych, "Accelerated 2D-IR using compressed sensing," J. Phys. Chem. Lett. **4**(15), 2489–2492 (2013).
[41]Z. Wang, S. Lei, K. J. Karki, A. Jakobsson, and T. Pullerits, "Compressed sensing for reconstructing coherent multidimensional spectra," J. Phys. Chem. A **124**(9), 1861–1866 (2020).
[42]J. Swärd, S. I. Adalbjörnsson, and A. Jakobsson, "High resolution sparse estimation of exponentially decaying $N$-dimensional signals," Signal Process. **128**, 309–317 (2016).
[43]M. E. Siemens, G. Moody, H. Li, A. D. Bristow, and S. T. Cundiff, "Resonance lineshapes in two-dimensional-Fourier transform spectroscopy," Opt. Express **18**(17), 17699–17708 (2010).
[44]A. Liu, S. T. Cundiff, D. B. Almeida, and R. Ulbricht, "Spectral broadening and ultrafast dynamics of a nitrogen-vacancy center ensemble in diamond," Mater. Quantum Technol. **1**, 025002 (2021).
[45]A. Liu, "An exact expression for multidimensional spectroscopy of a spin-boson Hamiltonian," Adv. Quantum Technol. **7**(3), 2300399 (2024).
[46]A. Liu, D. B. Almeida, W.-K. Bae, L. A. Padilha, and S. T. Cundiff, "Simultaneous existence of confined and delocalized vibrational modes in colloidal quantum dots," J. Phys. Chem. Lett. **10**(20), 6144–6150 (2019).
[47]Y. Laplace and A. Cavalleri, "Josephson plasmonics in layered superconductors," Adv. Phys.: X **1**(3), 387–411 (2016).
[48]A. Liu, "Off-axis imaging with off-axis parabolic mirrors," Appl. Opt. **62**(32), 8574–8576 (2023).